

Sputtered Ruthenium Oxide Neural Stimulation Electrodes *

Bitan Chakraborty, Alexandra Joshi-Imre, *Member, IEEE* and Stuart F. Cogan, *Member, IEEE*

Abstract— We have investigated the charge-injection properties of sputtered ruthenium oxide (RuO_x) coatings deposited on planar microelectrode arrays. Substantial charge was found to be available for injection within $-0.6/0.6$ V vs $\text{Ag}|\text{AgCl}$ potential limits for the sputtered RuO_x film. The charge-injection capacity increased further upon extending the potential limits to $-0.7/0.7$ V vs $\text{Ag}|\text{AgCl}$. No oxygen reduction, an unwanted side reaction, was observed during the pulsing of sputtered RuO_x microelectrodes in phosphate buffered saline solution. Additionally, the RuO_x coatings were found to be electrochemically stable for up to 1-billion-cycles of constant current stimulation pulsing at 8 nC/phase in model-ISF at 37° C.

Clinical Relevance— This work establishes RuO_x as high-charge-injection capacity and electrochemically stable electrode coating, with potential use for clinical neuromodulation.

I. INTRODUCTION

Microelectrode arrays are employed for restoring lost or impaired physiological functions and treatment of neurological disorders in humans. Electrodes are an integral part of such devices and must form a chronically stable interface with tissue. Safe electrical stimulation at the electrode-tissue interface is required and hence there is a need for high-charge-injection electrode materials capable of injecting relevant amounts of charge into the tissue.

Previously, we have developed a process for depositing sputtered ruthenium oxide films (RuO_x), using water vapor as one of the plasma constituents, as an electrode coating for neural stimulation and recording. [1] This film was also determined to be non-cytotoxic towards cortical neurons in a study of live/dead cells assays as well as through functional neurotoxicity studies. [2] In this study, we explored the stimulation charge-injection stability of sputtered RuO_x films deposited using previously established deposition conditions. [1] The safe operating potential window for sputtered RuO_x was established by slow sweep rate (50 mV/s) cyclic voltammetry in an inorganic model of interstitial fluid (model-ISF) at 37° C. Surface reduction of oxygen is common for platinum group metals, which produces noxious side products that are harmful to the tissue. [3] Therefore, we have evaluated the possibility of oxygen reduction during stimulation with sputtered RuO_x electrodes in buffered saline solution. Finally, the long-term electrochemical stability of the RuO_x films was assessed by constant current stimulation pulsing at 8 nC/phase (40 μA , 200 μs) in model-ISF at 37° C.

*Research supported by NIH grant 5R01NS104344-02.

B. Chakraborty is with the Materials Science and Engineering Department at The University of Texas at Dallas, Richardson, TX 75080 USA (e-mail: bitan.chakraborty@utdallas.edu).

II. METHODS

A. Ruthenium Oxide Sputter Deposition

An AJA ATC 2200 DC magnetron sputtering system (AJA Internationals, Scituate MA) was used to reactively sputter RuO_x films from 99.9% Ru metal targets. A mass-flow control system was used to introduce and maintain the flow rates of process gases, namely argon (Ar) at 20 sccm, oxygen (O_2) at 7.5 sccm and water vapor (H_2O) at 22.7 sccm. The process pressure was maintained at 30 millitorr. Planar circular microelectrode arrays with electrode sites of 50 μm diameter (~ 1960 μm^2 geometric surface area, GSA) were defined using photolithography, as described previously. [1] Fig. 1 shows a scanning electron microscopy (SEM) image of sputtered RuO_x electrodes.

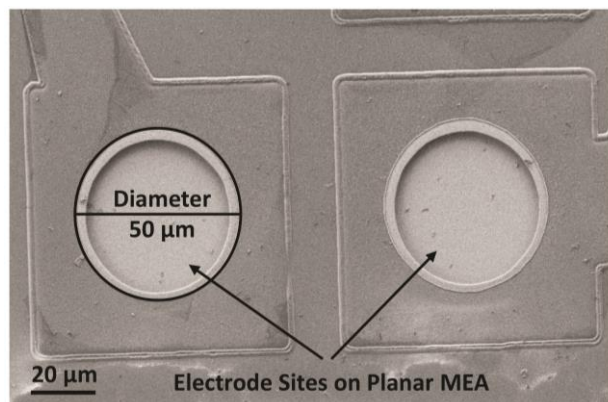


Figure 1. Scanning electron microscopic image of the electrode sites (50 μm diameter, ~ 1960 μm^2 GSA) consisting of sputtered RuO_x coatings in a planar microelectrode array (MEA).

B. Electrochemical Characterizations

Cyclic voltammetry (CV) and voltage transient measurements (VTMs) were performed in order to electrochemically characterize the sputtered RuO_x electrodes. A three-electrode set-up consisting of the RuO_x working electrode, a $\text{Ag}|\text{AgCl}$ reference electrode and a large surface area Pt wire counter electrode were employed for electrochemistry. A Gamry Reference 600 potentiostat was used for CV measurements and a Sigenics stimulator (Chicago, IL) was used for VTMs. The electrolytes consisted of phosphate buffered saline (PBS) solution and an inorganic model of interstitial fluid (model-ISF), prepared in the laboratory.

A. Joshi-Imre is with the Department of Research at The University of Texas at Dallas, Richardson, TX 75080 USA (e-mail: Alexandra.joshi-imre@utdallas.edu).

S. F. Cogan is with the Department of Bioengineering at The University of Texas at Dallas, Richardson, TX 75080 USA (corresponding author: phone: 972-883-4639; e-mail: stuart.cogan@utdallas.edu).

The PBS consisted of 130 mM NaCl, 22 mM $\text{NaH}_2\text{PO}_4 \cdot 7\text{H}_2\text{O}$, and 81 mM $\text{Na}_2\text{HPO}_4 \cdot \text{H}_2\text{O}$. The pH of PBS was measured to be ~ 7.2 and all the experiments using PBS were performed at room temperature ($\sim 20^\circ\text{C}$). The model-ISF was composed of 110 mM NaCl, 28 mM NaHCO_3 , 7.5 mM KHCO_3 , 2 mM $\text{Na}_2\text{HPO}_4 \cdot 7\text{H}_2\text{O}$, and 0.5 mM each of $\text{NaH}_2\text{PO}_4 \cdot \text{H}_2\text{O}$, MgSO_4 , MgCl_2 , and CaCl_2 . The pH of this electrolyte was maintained at ~ 7.4 by continuously flowing mixed gas (5% CO_2 , 6% O_2 , 89% N_2) through the solution. During experiments with model-ISF the temperature was maintained at 37°C .

C. Oxygen Reduction

The waveforms used in most neural stimulation protocols consists of a biphasic pulse where the leading phase is cathodal. During the cathodal phase the electrodes are polarized negatively to potentials at which oxygen reduction can occur at the surface of the electrode. The reactive species formed due to oxygen reduction have been identified as potentially toxic to tissue. [3,4] The contribution of oxygen reduction towards charge-injection during stimulation from sputtered RuO_x electrodes was determined by performing CVs and VTMs in phosphate buffer saline (PBS) solutions. First, the PBS was sparged with argon for 60 minutes to remove all dissolved oxygen. Argon was continuously flowed over the surface of the PBS during the electrochemical measurements in argon-saturated PBS (Ar/PBS). To assess a possible contribution from oxygen reduction to charge-injection, the PBS solution was sparged with oxygen for 60 mins, such that the solution is saturated with oxygen (O_2/PBS). O_2 was continuously flowed over the surface of the PBS during electrochemical measurements in O_2/PBS .

D. Constant Current Stimulation

The long-term electrochemical stability of the sputtered RuO_x electrodes was evaluated by performing constant-current stimulation with rectangular biphasic pulses in model-ISF maintained at 37°C . The current waveform was generated using a PlexStim 16-channel stimulator (Plexon, Dallas, TX), and consisted of a cathodal first pulse of 40 μA amplitude and 200 μs duration, an interphase delay of 100 μs , and an anodal pulse of same magnitude as the first pulse. A frequency of 200 Hz was maintained such that ~ 1 billion pulses were attained over 9 weeks. The voltage transient, CV and EIS measurements were collected weekly to monitor changes in electrochemical performance of the pulsed electrodes overtime.

E. Statistical Analysis

Data sets were tested for normality using the Shapiro-Wilk method with a level of significance $\alpha = 0.05$. All normally distributed data sets, measured from electrodes of the same array, were reported as mean \pm standard deviation (SD). Two-sided paired t-tests ($\alpha = 0.05$) were performed to compare between parameters.

A. Water Electrolysis Window

Water electrolysis limits were established from CVs in model-ISF as shown in Fig. 2. The onset of water reduction and oxidation is indicated by the abrupt increase in current observed at the negative and positive potential limits, respectively, at -0.9 V and 0.9 V vs Ag/AgCl . The large current-onset is attributed to water electrolysis reaction [5]. These current increases are not observed at -0.8 V and 0.8 V potential limits. Therefore, the potential limits that avoid water electrolysis by RuO_x were set at -0.8 V and 0.8 V . These potential limits are similar to those established previously for sputtered iridium oxide (SIROF) although the water reduction potential for RuO_x is 100 mV more negative than that typically quoted for SIROF. [6]

For comparison with SIROF electrodes, the more conservative potential limits of -0.6 V and 0.8 V vs Ag/AgCl were chosen to allow more direct comparison. Therefore, most of the analysis was based on CVs with -0.6 V to 0.6 V scan range. The cathodal charge storage capacity (CSC_c) was calculated using time integral of the cathodal current over the $-0.6/0.6\text{ V}$ range CVs at 50 mV/s and 50,000 mV/s scan rates. Similarly, the stimulation charge densities are also based on the $-0.6/0.6\text{ V}$ potential limits.

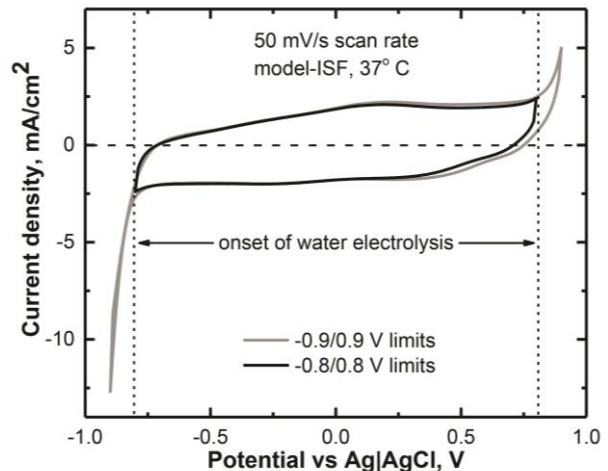


Figure 2. Comparison between cyclic voltammograms of the same electrode taken over a scan range of -0.9 V to 0.9 V and -0.8 V to 0.8 V , showing the water electrolysis window as indicated by high current onsets.

B. Oxygen Reduction

CVs of sputtered RuO_x microelectrodes of $\sim 1960\ \mu\text{m}^2$ GSA were performed in Ar/PBS and O_2/PBS and are compared in Fig. 3. Slow-sweep rate CVs taken at 50 mV/s for RuO_x electrodes (mean \pm SD, $n=4$) in Ar/PBS and O_2/PBS are shown in Fig. 3a. In O_2/PBS a significant increase in negative current is observed at potentials more negative than -0.2 V . This additional cathodal current is attributed to reduction of oxygen and is similar to that observed for SIROF electrode of similar dimension. [6] The CSC_c (mean \pm SD, $n=4$) of the RuO_x microelectrodes in O_2/PBS was calculated to be $51.88 \pm 0.57\text{ mC}/\text{cm}^2$ compared to $40.90 \pm 0.17\text{ mC}/\text{cm}^2$ for CVs measured in Ar/PBS. This suggests that oxygen reduction at the RuO_x surface contributes to about $10.99 \pm 0.40\text{ mC}/\text{cm}^2$ or

~27% of the charge admittance during negative potential sweeps at 50 mV/s.

Minimal change was observed for the CVs at 50,000 mV/s sweep rate for the same set of four electrodes when compared in Ar/PBS and O₂/PBS, as shown in Fig. 3b. Specifically, at the negative potentials, relevant to oxygen reduction, almost no change in current magnitudes was observed from the averaged CVs (mean ± SD, n=4) measured in Ar/PBS and O₂/PBS. The CSC_C values calculated from the CVs at 50,000 mV/s were 9.67 ± 0.20 mC/cm² and 9.85 ± 0.11 mC/cm² in Ar/PBS and O₂/PBS respectively. This result suggests that short periods of negative electrode potentials will not reduce a significant amount of oxygen during current pulsing. A similar result was also observed for SIROF electrodes of similar GSA. [7]

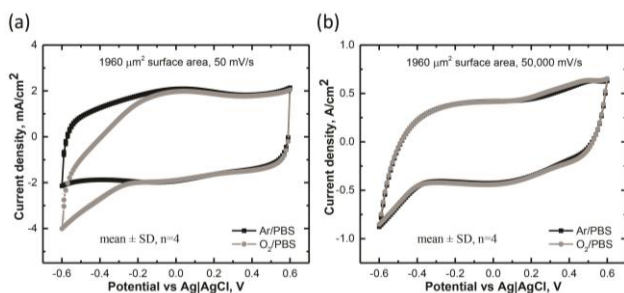


Figure 3. Cyclic voltammograms of a sputtered RuO_x electrodes in argon and oxygen saturated PBS showing contribution of oxygen reduction. (a) CVs at 50 mV/s scan rate. (b) CVs at 50,000 mV/s scan rate.

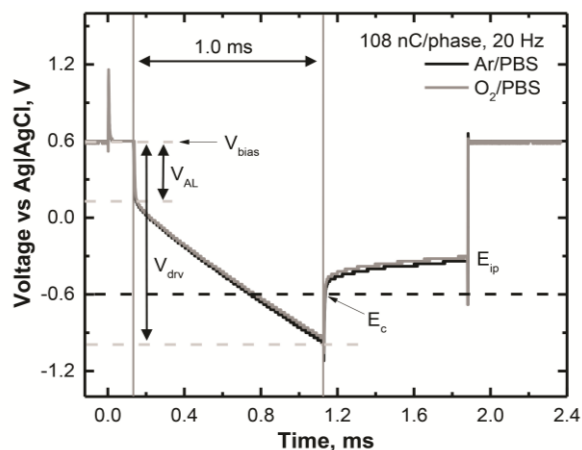


Figure 4. Comparison of the voltage transient response of a sputtered RuO_x electrode in argon and oxygen saturated PBS measured at 108 nC/phase with 20 pulses per second.

TABLE I. COMPARISON OF DIFFERENT PARAMETERS FROM VOLTAGE TRANSIENT MEASUREMENTS OF PLANAR RUTHENIUM OXIDE MICROELECTRODES IN OXYGEN AND ARGON SATURATED PBS

	Ar/PBS	O ₂ /PBS
V _{drv} , V	1.58 ± 0.06	1.58 ± 0.07
V _{AL} , V	0.46 ± 0.02	0.45 ± 0.02
E _c , V	-0.54 ± 0.04	-0.53 ± 0.06
E _{ip} , V	-0.36 ± 0.04	-0.35 ± 0.04

We further investigated the occurrence of oxygen reduction during stimulation by voltage transient measurements in Ar/PBS and O₂/PBS as shown in Fig. 4. The electrode was subjected to current pulses with 108 μA amplitude and 1.0 ms pulse duration (108 nC/phase) at 20 pulses per second repetition rate. The voltage transient response from this current pulse, shown in Fig. 4, is an average from 64 pulses. From these voltage transients, the driving voltage, V_{drv}, the leading access voltage, V_{AL}, the cathodal potential excursion, E_c and the inter-pulse end potential E_{ip} were determined (Table 1). The V_{drv} obtained from voltage transients in Ar/PBS was 1.58 ± 0.06 V and in O₂/PBS was 1.58 ± 0.07 V. These values were found to be not statistically significant (p=0.30, n=5). The E_c in Ar/PBS and O₂/PBS were respectively -0.54 ± 0.04 V and -0.53 ± 0.06 V and were not statistically significant (p=0.99, n=5). The other parameters, V_{AL} and E_{ip} were also found to be not statistically significant. Therefore, no effect of oxygen reduction was observed during stimulation of RuO_x electrodes with 1.0 ms pulse duration, which is consistent with cyclic voltammetry measurements at 50,000 mV/s.

C. Potential Limit Effects on Charge-Injection

The effect of expanding potential limits on the maximum charge-injection capacity of RuO_x were evaluated. Based on the CV data from Fig. 2, we investigated charge-injection using a 0.7 V interpulse bias and a -0.7 V maximum cathodal potential excursion.

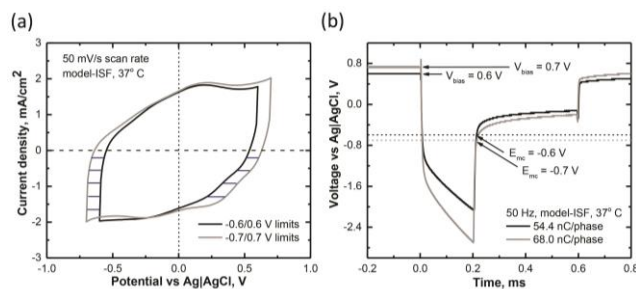


Figure 5. Comparison of charge availability when the potential window is increased from -0.6/0.6 V to -0.7/0.7 V vs Ag/AgCl in model-ISF at 37° C for RuO_x film (160 nm thickness). (a) CV showing the additional charge (shaded region) available upon increasing the potential window. (b) Corresponding charge in voltage transient response upon increasing the bias from 0.6 V to 0.7 V and as well as the E_{mc} from -0.6 V to -0.7 V.

TABLE II. COMPARISON OF CHARGE DENSITY FOR SPUTTERED RUTHENIUM OXIDE (160 NANOMETERS THICKNESS) MICROELECTRODES USING 0.6 V AND 0.7 V BIAS AND CATHODAL LIMITS OF -0.6 V AND -0.7 V.

Bias vs Ag/AgCl (V)	0.60	0.70
	Charge density (mean ± SD, n=4)	
E _{mc} limit (V)	mC/cm ²	
-0.60	2.92 ± 0.92	3.18 ± 0.04
-0.70	3.22 ± 0.05	3.44 ± 0.05

Fig. 5a shows the CV of a sputtered RuO_x electrode with a -0.7/0.7 V water window in comparison to a CV with -0.6/0.6

V window. The shaded regions indicate the additional charge that may be accessed by increasing the potential window. This corresponds to 8.14 ± 0.55 mC/cm² (mean \pm SD, n = 4) or $\sim 25\%$ increase in the charge storage capacity. Consequently, as shown in Fig. 5b, we obtained the voltage-transient response of the electrode by increasing the anodal interpulse bias to 0.7 V and the maximum negative electrode potential to -0.7 V. The charge density values as a result of increasing either the bias or the E_{mc} or both compared to the set values (mean \pm SD, n = 4) are tabulated in Table 2. The charge density increased from 2.92 ± 0.92 mC/cm² (57.2 ± 1.8 nC/phase) to 3.44 ± 0.05 mC/cm² (67.4 ± 1.0 nC/phase) upon increasing both bias and the E_{mc} value, as shown in Table 2. This amounts to $\sim 18\%$ increase in charge density upon extending the potential limits for stimulation in model-ISF at 37° C. The charge injection capacity of the sputtered RuO_x also depends on the film thickness. In a previous study, we reported the approximately linear increase in charge density over 120-630 nm film thickness from ~ 4.4 -11.4 mC/cm² in phosphate buffered saline at 0.6 V bias vs Ag|AgCl. [8]

D. Constant Current Stimulation Stability

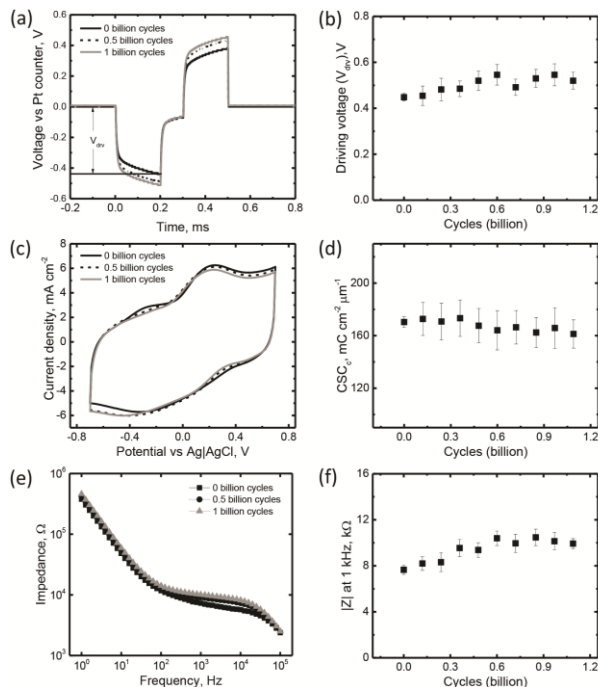


Figure 6. Constant current stimulation stability of sputtered RuO_x in model-ISF at 37° C under 1 billion-cycle at 8 nC/phase. (a) Representative voltage transients. (b) Representative cyclic voltammograms at 50 mV/s. (c) Representative electrochemical impedance spectra. (d) Weekly monitoring of V_{drv} (mean \pm SD, n = 5). (e) Weekly monitoring of CSC_c (mean \pm SD, n = 5). (f) Weekly monitoring of impedance at 1 kHz (mean \pm SD, n = 5).

In model-ISF at 37° C, the stability of the RuO_x coatings for long-term current pulsing was assessed in response to 8 nC per phase (0.4 mC/cm²) biphasic current pulses. Voltage transients recorded periodically during pulsing showed a slight increase in maximum driving voltage, V_{drv} at 1 billion pulses (9 weeks) as shown in Figure 6a. The V_{drv} determined from the

voltage transients also showed a slight increase over time up to 1 billion cycles, as shown in Figure 6b.

Figures 6c and e show representative CVs at 50 mV/s and EIS Bode plots respectively for a pulsed electrode. The corresponding CSC_c and 1 kHz impedance magnitude, averaged over all pulsed electrodes, are shown in Figures 6d and 6f, respectively, over the 1 billion pulses. No significant change in CSC_c and a slight increase in 1 kHz impedance was observed, as shown in Figure 6e and f. The change might be associated with microstructural change in the film or salt accumulation on the electrode sites during pulsing. Further investigation is required to understand this observation. However, the observed changes in electrochemical response of the RuO_x electrodes are modest and do not reveal obvious film degradation. The sputtered RuO_x films were found to be electrochemically stable for up to 1 billion pulses at 8 nC/phase in model-ISF at 37° C.

IV. CONCLUSION

Electrochemical properties of sputtered ruthenium oxide coatings were investigated for their application as neural stimulation electrodes. The sputtered RuO_x electrodes were found to be stable for up to 1 billion cycles of stimulation pulsing in model-ISF at 37° C. Our results suggest that sputtered RuO_x films are an excellent candidate for chronic neural stimulation electrode coatings and warrant further investigations. At present, implantable microelectrode arrays coated with sputtered RuO_x are being fabricated for investigating chronic stability in pre-clinical animal models to understand the effects of biomolecule interactions during stimulation charge injection.

REFERENCES

- [1] B. Chakraborty, A. Joshi-Imre, J. Maeng, and S. F. Cogan, "Sputtered ruthenium oxide coatings for neural stimulation and recording electrodes," *J. Biomed. Mater. Res. Part B Appl. Biomater.*, vol. 109, no. 5, pp. 643-653, August 2021.
- [2] R. Atmaramani, B. Chakraborty, R. T. Rihani, J. Usoro, A. Hammack, J. Abbott, P. Nnoromele, B. J. Black, J. J. Pancrazio, and S. F. Cogan, "Ruthenium oxide based microelectrode arrays for in vitro and in vivo neural recording and stimulation," *Acta biomaterialia* 101, pp. 565-574, 2020.
- [3] S. L. Morton, M. L. Daroux, and J. T. Mortimer, "The role of oxygen reduction in electrical stimulation of neural tissue," *J. Electrochem. Soc.*, 141, no. 1, pp. 122, 1994.
- [4] S. L. Morton, M. Daroux, and J. T. Mortimer, "The role of oxygen reduction in electrical stimulation of nervous tissue," *Proc. Annu. Conf. Eng. Med. Biol.*, vol. 13, no. pt 2, pp. 552-553, 1991.
- [5] S. F. Cogan, "Neural stimulation and recording electrodes," *Annu. Rev. Biomed. Eng.*, vol. 10, pp. 275-309, 2008.
- [6] S. F. Cogan, J. Ehrlich, T. D. Plante, A. Smimov, D. B. Shire, M. Gingerich, and J. F. Rizzo, "Sputtered iridium oxide films for neural stimulation electrodes," *J. Biomed. Mater. Res. Part B Appl. Biomater.*, vol. 89B, no. 2, pp. 353-361, May 2009.
- [7] S. F. Cogan, J. Ehrlich, T. D. Plante, M. D. Gingerich, and D. B. Shire, "Contribution of oxygen reduction to charge injection on platinum and sputtered iridium oxide neural stimulation electrodes," *IEEE Trans. Biomed. Eng.*, vol. 57, no. 9, pp. 2313-2321, 2010.
- [8] B. Chakraborty, A. Joshi-Imre, and S. F. Cogan, "Charge injection characteristics of sputtered ruthenium oxide electrodes for neural stimulation and recording," *J. Biomed. Mater. Res. Part B Appl. Biomater.*, 1-10, 2021. <https://doi.org/10.1002/jbm.b.34906>.